

ARTICLE TYPE

Constraining the Evolution of the H_I Spin Temperature with Fast Radio Bursts

H. Roxburgh,¹ M. Glowacki,^{1,2} A. Bera,^{1,3} and C. W. James¹

¹International Centre for Radio Astronomy Research, Curtin University, Bentley, WA 6102, Australia

²Institute for Astronomy, University of Edinburgh, Royal Observatory, Edinburgh, EH9 3HJ, United Kingdom

³ASTRON, the Netherlands Institute for Radio Astronomy, Oude Hoogeveensedijk 4, 7991 PD Dwingeloo, The Netherlands

Author for correspondence: H. Roxburgh, Email: hugh.roxburgh@postgrad.curtin.edu.au.

Abstract

Fast radio bursts (FRBs) emit broad band radio wave radiation that may, in rare cases, encode atomic hydrogen (H_I) absorption signals produced as they traverse the interstellar medium of their host galaxies. Combining such signals with high resolution H_I emission maps offers a unique opportunity to probe the dynamics of neutral gas at cosmological distances through constraints of the H_I excitation temperature T_{spin} , which characterises the balance of neutral gas phases and the underlying thermal processes within these galactic environments. While no absorption signal has been recorded in an FRB to date, we demonstrate a proof of concept with the bright ($F = 35$ Jy ms) and narrow (0.2 ms) FRB 20211127I detected by ASKAP. We find a 3σ upper limit on the integrated optical depth in the pulse-averaged spectrum of 33 km s^{-1} , and, based on the H_I emission observed in a 3 hr MeerKAT *L*-band observation, subsequently find a lower limit on T_{spin} of 26 K. While this test case provides little constraining power, we find that narrow, non-repeating FRBs with fluences greater than 20/70/150 Jy ms observed with all dishes with the current MeerKAT/ASKAP/DSA telescopes can probe integrated optical depths below 5 km s^{-1} . Furthermore, we highlight that utilising FAST's incredible sensitivity to stack thousands of bursts from hyperactive repeaters also provides a plausible avenue through which H_I absorption, and hence T_{spin} , can be measured. Finally, we discuss how H_I absorption can address several modern challenges in FRB science, providing a physical anchor for locating bursts within their host galaxies and helping to disentangle the host contribution to dispersion and scattering.

1. Introduction

Since its peak around redshift $z \sim 2$, the observed star formation rate density (SFRD) in the Universe has declined roughly tenfold (Hopkins and Beacom 2006; Madau and Dickinson 2014; Driver et al. 2018). This evolution of the cosmic star formation history (SFH) is largely attributed to the interplay between the gravitational infalling of matter onto galaxies and the expulsion of matter from galaxies due to various feedback processes (e.g. Cox and Smith 1974; McKee and Ostriker 1977; Gatto et al. 2015), though the driving factors surrounding this intricate cycle remain unclear.

It is well established that the baryons lying in the interstellar medium (ISM) exist in various phases of matter (Tielens 2005). The bulk of this material exists as atomic hydrogen gas (H_I) with temperatures ranging from a few hundred to a few thousand Kelvin. Through various radiative cooling processes, this gas can contract into clouds of molecular hydrogen (H₂) which are dense enough to gravitationally collapse into stars (Krumholz, McKee, and Tumlinson 2009). As such, a galaxy's H_I gas reservoir constitutes its star formation fuel, and thus its properties and dynamics are intrinsically tied to the rate of star formation.

While observations of the 21-cm emission line – which arises from the spin flip transition of atomic hydrogen – broadly reveal the bulk distributions and kinematics of H_I gas in galaxies, observations of our own Milky Way reveal that the reservoir can be further separated into distinct, coexisting phases

of H_I gas (McKee and Ostriker 1977; Heiles and Troland 2003; Wolfire et al. 2003). The cooler, denser material forms what is called the cold neutral medium (CNM) at temperatures around 100 K, whilst hotter material forms a diffuse warm neutral medium (WNM) around 10,000 K. These are stable phases of matter, though an unstable bridging phase also exists around 500 K, produced through shocks in the ISM (Murray et al. 2018). The interaction between these phases of matter plays an integral role in galaxy evolution (McKee and Ostriker 1977), and thus understanding how it varies over cosmic time and how it relates to particular galactic feedback processes – such as those from supernovae (SNe) and active galactic nuclei (AGN) winds – is a critical field of inquiry.

Probing the nature of the physical conditions that differentiate these gas phases in galaxies is challenging. Studies focused on the absorption of background emission by foreground atomic hydrogen is considered one of the most effective methods through which to infer deeper information on the phase dynamics (Allison 2021). In particular, the equivalent width of the H_I absorption line is directly connected to the population ratio between atoms in the two hyperfine spin states, through the effective excitation or "spin" temperature, T_{spin} . This variable quantifies the population ratio, and in the cold dense gas of the CNM, it is considered a solid proxy for the gas' bulk kinetic temperature, T_k , as atomic collisions are common enough for the weak spontaneous H_I transition to occur (Roy et al. 2013).

Measuring T_{spin} , however, presents its own challenges. Given T_{spin} quantifies a population ratio, one must know the total column density along the line of sight, N_{HI} , to explicitly measure it. This limits true constraints on T_{spin} to be made from only the rare cases where the bulk H_I gas density along the line of sight is known, either through Ly- α absorption of the background source (e.g. Curran *et al.* 2010; Kanekar *et al.* 2014), or, in a few cases, through direct detection of H_I emission from the foreground galaxy (e.g. Reeves *et al.* 2016; N. Gupta *et al.* 2018). Both approaches depend on the presence of a background-quasar/foreground-galaxy pair, which occurs only rarely.

However, the discovery of a bright extragalactic population of fast radio bursts (FRBs) over the past decade (Lorimer *et al.* 2007; Thornton *et al.* 2013) may provide a far more powerful means of directly measuring extragalactic T_{spin} . While the nature of their progenitors remains elusive, FRB signals can theoretically encode H_I absorption from the ISM of their host galaxies (Fender and Oosterloo 2015; Margalit and Loeb 2016); combining this with highly resolved H_I emission maps thus offers a direct measurement of T_{spin} in their hosts. Given their detection beyond $z = 2$ (Caleb *et al.* 2025), and with hundreds of events occurring across the sky each day (CHIME/FRB Collaboration *et al.* 2021), FRBs could enable a substantially expanded, redshift-dependent census of T_{spin} over cosmic history.

In this paper, we explore a proof of concept for constraining the evolution of the H_I spin temperature over cosmic time using FRBs. In Section 2, we cover the theory through which T_{spin} is measured from H_I emission and absorption signals, and introduce our methodology for doing so with FRBs. In Section 3, we explore a proof of concept with a real FRB whose host has been observed in H_I emission. In Section 4, we discuss the outlook for H_I absorption and constraining T_{spin} using FRBs moving forward, and conclude in Section 5.

2. Theory

2.1 Deriving T_{spin}

In an H_I gas reservoir, the relative population of atoms in the lowest singlet hyperfine state and the higher triplet hyperfine state ($F = 0, 1$ respectively, where F is the total angular momentum quantum number) is determined using the Boltzmann distribution, and is expressed

$$\frac{n_2}{n_1} = \frac{g_2}{g_1} \exp\left(\frac{-\Delta E}{kT_{\text{spin}}}\right), \quad (1)$$

where g is the state degeneracy, ΔE is the energy difference between the two states, and k is Boltzmann's constant. This effective temperature directly impacts how opaque a medium is to the 21-cm signal; if most atoms are in the singlet state, the optical depth is much higher as absorption is more likely to occur.

The optical depth of a medium can be measured from the absorption spectra of a source. If the continuum emission flux

density is denoted S_c , then the frequency dependent optical depth of an absorption feature can be found using

$$\tau(\nu) = -\ln\left(1 - \frac{\Delta S(\nu)}{f_c S_c}\right), \quad (2)$$

where ΔS is the difference between S_c and the minimum of the absorption line, and f_c is the covering fraction — the fraction of the background source covered by the foreground absorber on the sky. As FRBs are extremely physically compact sources ($r \sim 10$ km, Farah *et al.* 2018), f_c is always equal to unity, so we drop it henceforth. For optically thin emission ($\tau \ll 1$), this becomes

$$\tau(\nu) \simeq \frac{\Delta S(\nu)}{S_c}. \quad (3)$$

One can then calculate the total column density of H_I atoms along the line of sight using (e.g. Wilson, Rohlfs, and Hüttemeister 2013):

$$N_{\text{HI}} = 1.823 \times 10^{18} T_{\text{spin}} \int \tau(\nu) d\nu \text{ cm}^{-2}. \quad (4)$$

This expression can thus easily be rearranged to calculate T_{spin} given a measurement of N_{HI} from H_I emission, and $\tau(\nu)$ from H_I absorption.

2.2 H_I Absorption in FRBs

The morphologies of FRB signals are highly varied (e.g. Plenunis *et al.* 2021), though a good fraction of the population emit broad-band radiation. Many signals overlap with the frequency range of interest for studies of the H_I transition, which has its rest frequency, ν_{HI} , at ~ 1420 MHz. As such, it is plausible that FRBs may encode an absorption signal associated with the redshifted frequency of the H_I transition in its host galaxy.

Both Fender and Oosterloo (2015) and Margalit and Loeb (2016) explored this concept in the early days of the field, when just a handful of FRBs had been detected. Their focuses were on using the redshift of a potential absorption line as a distance estimator, as no FRB had been localised to its host galaxy yet. Furthermore, the establishment of the repeating subclass of FRBs was very new (Spitler *et al.* 2016), and neither paper explored in detail the very interesting possibilities such objects offer through stacking methods, which we discuss later. It is therefore worth revisiting the theory of detecting absorption in the signals of FRBs.

An FRB's sensitivity to absorption detection is solely dependent on the signal-to-noise ratio (SNR) of its spectrum averaged over its temporal pulse width w_{FRB} at a spectral resolution of ΔV in velocity space. Defining σ_ν as the 1σ uncertainty on the FRB flux density at each frequency channel, and σ_τ as the corresponding 1σ uncertainty on the derived optical depth, Eq. 3 can then be written as

$$\sigma_\tau = \frac{\sigma_\nu}{S_{\text{FRB,HI}}} = \frac{1}{\text{SNR}_{\text{FRB,HI}}}. \quad (5)$$

Here, the subscript emphasises that this is the spectral SNR measured at the location of the $\text{H}\alpha$ line. This is not the same SNR as is reported in FRB discovery papers, which relates to the temporal pulse profile instead. Therefore, while we stress that SNR is the sole deciding factor in an FRB's sensitivity to absorption, if we wish to estimate the sensitivities probed by the current population of detected FRBs, we must expand this expression in terms of their reported properties and those of the theoretical absorption features.

For a resolved absorption line with a width W spanning N channels of velocity width ΔV , the integrated optical depth is given by

$$\int \tau = \sum_i^N \tau_i \Delta V \text{ km s}^{-1}. \quad (6)$$

Assuming uncorrelated noise, the uncertainty adds in quadrature:

$$\begin{aligned} \sigma_{\int \tau}^2 &= \text{Var} \left(\sum_i^N \tau_i \Delta V \right) = \sum_i^N \Delta V^2 \text{Var}(\tau_i) \\ &= N \Delta V^2 \sigma_{\tau}^2 = W \Delta V \sigma_{\tau}^2. \end{aligned} \quad (7)$$

The noise in the pulse-averaged spectrum can be derived from the radiometer equation:

$$\begin{aligned} \sigma_{\nu} &= \frac{\text{SEFD}}{\sqrt{N_{\text{pol}} w_{\text{FRB}} \Delta \nu}} \text{ Jy} \\ &= \text{SEFD} \sqrt{\frac{c}{\nu_{\text{HI}}}} \sqrt{\frac{1+z}{N_{\text{pol}} w_{\text{FRB}} \Delta V}} \text{ Jy}, \end{aligned} \quad (8)$$

after transforming into the FRB's rest frame velocity space using its redshift z . Using this expression and Eq. 7, we arrive at the sensitivity to integrated optical depth in terms of a telescope's SEFD, the line width, and an FRB's properties:

$$\begin{aligned} \sigma_{\int \tau} &= \sigma_{\tau} \sqrt{W \Delta V} = \frac{\sigma_{\nu} \sqrt{W \Delta V}}{S_{\text{FRB,HI}}} \\ &= \frac{\text{SEFD}}{S_{\text{FRB,HI}}} \sqrt{\frac{c}{\nu_{\text{HI}}}} \sqrt{\frac{W (1+z)}{N_{\text{pol}} w_{\text{FRB}}}} \text{ km s}^{-1}. \end{aligned} \quad (9)$$

The final simplification we can incorporate deals with the spectral behaviour of FRBs, which can be complex; some bursts occupy only part of the observing bandwidth (Pleunis et al. 2021), and others encode interstellar scintillation such that even bright bursts may show little flux at the $\text{H}\alpha$ line (Mausi et al. 2015). However, while there is some evidence for a preference toward lower-frequency emission (James et al. 2022; Shin et al. 2023; Shannon et al. 2024), no strong systematic trend in flux density is observed across the narrow bandwidth relevant here. For simplicity, and following several previous studies (CHIME/FRB Collaboration et al. 2021), we therefore can assume an idealised FRB with a flat spectrum, such that

$S_{\text{FRB,HI}}(\nu) = \bar{S}_{\text{FRB,HI}}(\nu)$. This can be expressed in terms of the FRB fluence, F_{FRB} , as

$$\bar{S}_{\text{FRB,HI}}(\nu) = \frac{F_{\text{FRB}}}{w_{\text{FRB}}},$$

which then allows Equation 9 to be helpfully rewritten as a fluence-dependent metric. Using this form, a 3σ limit is equal to

$$L_{3\sigma} = \frac{3 \times \text{SEFD}}{F_{\text{FRB}}} \sqrt{\frac{c}{\nu_{\text{HI}}}} \sqrt{\frac{W w_{\text{FRB}} (1+z)}{N_{\text{pol}}}} \text{ km s}^{-1}. \quad (10)$$

2.3 Measuring T_{spin} & Beam Size

It is important to briefly consider the scales being probed through both $\text{H}\alpha$ emission and absorption in this context, and what that means for the interpretation of the measured T_{spin} . Most direct T_{spin} measurements are made by observing the $\text{H}\alpha$ and Lyman- α absorption of a foreground galaxy in the spectrum of a background QSO, though there are a few cases where the column density measurement has been derived from $\text{H}\alpha$ emission maps as we attempt here (e.g. Reeves et al. 2016; N. Gupta et al. 2018). This method is largely required for probing low redshift ($z < 1$) gas; the rest wavelength of the Ly- α line lies in the ultraviolet (UV), a regime which the Earth's atmosphere is opaque to.

These studies acknowledge that the scale over which the absorption occurs — i.e. the physical size of the absorbing region in the foreground galaxy — is much smaller than the angular resolution of the telescopes used to probe $\text{H}\alpha$ emission. However, they stress that the measured T_{spin} value is a column density weighted harmonic mean temperature, which describes the broader thermal state of the galaxy's ISM in the region around the absorber, rather than any individual cloud intersected along the line of sight.

Given FRBs are effectively point sources, they probe only the gas the pencil beam traverses, and thus any derived T_{spin} measurement is a harmonic mean of the surrounding medium. Particularly in face-on galaxies, where any line of sight through the disk intersects a relatively short path length and the emitting gas sampled by the beam arises from a similar physical region of the disk, the beam-averaged $\text{H}\alpha$ emission provides a reasonable proxy for the column density associated with the absorbing material. In this geometry, small-scale variations in cloud structure occur primarily side-by-side across the disk rather than being stacked along the line of sight. This prevents the signal from being distorted by multiple overlapping layers of gas, and therefore the large-scale emission map provides a much cleaner reflection of the specific environment the FRB passes through.

3. Analysis

We now attempt to demonstrate a proof of concept with real FRBs and $\text{H}\alpha$ intensity maps of their host galaxies. Over 100 FRBs have been localised to their host galaxies, a good fraction

at arcsecond scales (Shannon et al. 2024; Sharma et al. 2024; CHIME/FRB Collaboration et al. 2025; Pastor-Marazuela et al. 2025). Until recently, only a handful of these hosts had been studied individually for their H_I content (Michałowski 2021; Kaur, Kanekar, and Prochaska 2022; Glowacki et al. 2023; Lee-Waddell et al. 2023; Glowacki et al. 2024; Kaur, N, and Prochaska 2025). However, Roxburgh et al. (2025) expanded the sample to 22 hosts, providing the first population-level analysis through new observations with MeerKAT (Jonas and The MeerKAT Team 2016), the Giant Metrewave Radio Telescope (GMRT; Swarup et al. 1991; Y. Gupta et al. 2017), and the Five-hundred-meter Aperture Spherical Telescope (FAST; Nan et al. 2011). The majority of these detections were resolved, offering insights into the spatial distribution of gas in FRB host galaxies.

Candidate FRBs for this proof of concept must satisfy five requirements:

1. They must have spectra captured at very high spectral resolution, at least around 10 km s⁻¹ to unequivocally resolve any potential absorption line.
2. They must be localised to arcsecond or better precision to ensure the line of sight is well understood.
3. The redshift of their host galaxy must lie in the nearby Universe ($z < 0.1$) — this is due in part to the inherent weak intensity of the H_I emission line, but mostly due to the dominant radio frequency interference (RFI) that occupies frequencies until $z \sim 0.2$.
4. Their signals must have been detected in the frequency range of the redshifted H_I transition.
5. The H_I emission from their host galaxies should be bright and resolved in both spatial and spectral dimensions.

A tentative sixth requirement may include the host galaxy exhibiting low inclination (i.e. face-on) to mitigate line-of-sight confusion and beam-averaging effects in the associated H_I emission, thereby improving the interpretability of any derived T_{spin} measurement. However, higher inclination also increases the likelihood of absorption detection, so we do not consider this a strict requirement.

Of the options presented in Roxburgh et al. (2025), only one meets all these criteria: FRB 20211127I. This was detected by the Australian SKA Pathfinder (ASKAP; Hotan et al. 2021) telescope and analysed by Glowacki et al. (2023), Shannon et al. (2024), and Scott et al. (2025). In Figure 1, we present its dedispersed dynamic spectrum, which has been processed offline through the CELEBI (CRAFT Effortless Localisation and Enhanced Burst Inspection; Scott et al. 2023) pipeline. Alongside this, we display VLT imaging of its host galaxy with its localisation and the host's H_I emission overlaid as measured by MeerKAT.

Unfortunately, as is evident in the “striped” appearance of the FRB's signal in the dynamic spectrum, this FRB exhibits strong interstellar scintillation. Some FRBs show scintillation patterns with decorrelation bandwidths ν_{DC} — i.e. the scale over which scintillation fringes oscillate — near or equal to the characteristic widths of absorption features. Scott et al. (2025)

find a ν_{DC} of 2.9 MHz for this FRB, which corresponds to around 650 km s⁻¹ in the rest frame, and thus this is not a significant issue for this FRB. However, scintillation still makes discerning an absorption signal difficult; as shown by the horizontal line in the dynamic spectrum, the H_I line lies near the boundary of a scintle and a trough. Regardless, we can extract a high resolution spectrum around this region and search for absorption signals.

In Fig. 2, we present the H_I emission line spectrum arising from the pixel nearest the FRB's localisation region. We also show the same frequency range in the FRB's dedispersed signal, which has been flattened by fitting a local polynomial baseline, calculated while excluding all emission channels. Each spectrum is arbitrarily normalised here. We find that, as expected, no clear H_I absorption signal is present in the spectrum of FRB 20211127I. Instead, we calculate an upper limit on the strength of any potential H_I absorption, and use this to propagate through to a lower limit on T_{spin} .

If we assume an H_I line width W of 50 km s⁻¹ — which is broadly a representative width of H_I absorption features detected in spectra of extragalactic sources (Prochaska et al. 2008) — we can rebin the absorption spectrum such that our individual channel width is equal to W and measure the resulting noise level. As the spectrum is normalised, this noise level is simply the inverse of the spectral SNR outlined earlier, which we find to be equal to 5.9. This SNR is too low to use the simplifying expression presented in equation 3; reincorporating the log term into equation 10 gives our 3σ limit in the integrated optical depth of roughly 33 km s⁻¹.

We can now place a lower limit on T_{spin} using equation 3. To most accurately compare emission and absorption, we need to calculate our column density over the same line width we assume for our absorption profile. Given the width of the emission line at the pixel nearest the FRB location is roughly 170 km s⁻¹, we can construct an equivalent boxcar emission spectrum containing equal total flux and then integrate over just 50 km s⁻¹. This results in an H_I column density, N_{HI} , of $1.43 \times 10^{21} \text{ cm}^{-2}$. Combining this with our upper limit for the integrated optical depth, we find a 3σ lower limit for T_{spin} of roughly 26 K.

4. Discussion

As expected for non-detections in absorption, the result for this test case is unremarkable. The derived T_{spin} values from direct emission-absorption systems are in the hundreds of K (Reeves et al. 2016; N. Gupta et al. 2018), where interesting conclusions can be drawn about the dynamics of the CNM and WNM. Milky Way absorption finds typical lower limits for CNM cloud temperatures around 80 K (Murray et al. 2018); as such, our lower limit of 26 K provides little useful constraining power. However, there are a number of reasons to believe such a prescription will be viable moving forwards. Here, we comment on the specific pros and cons of this particular FRB, and the outlook of future FRB observation campaigns.

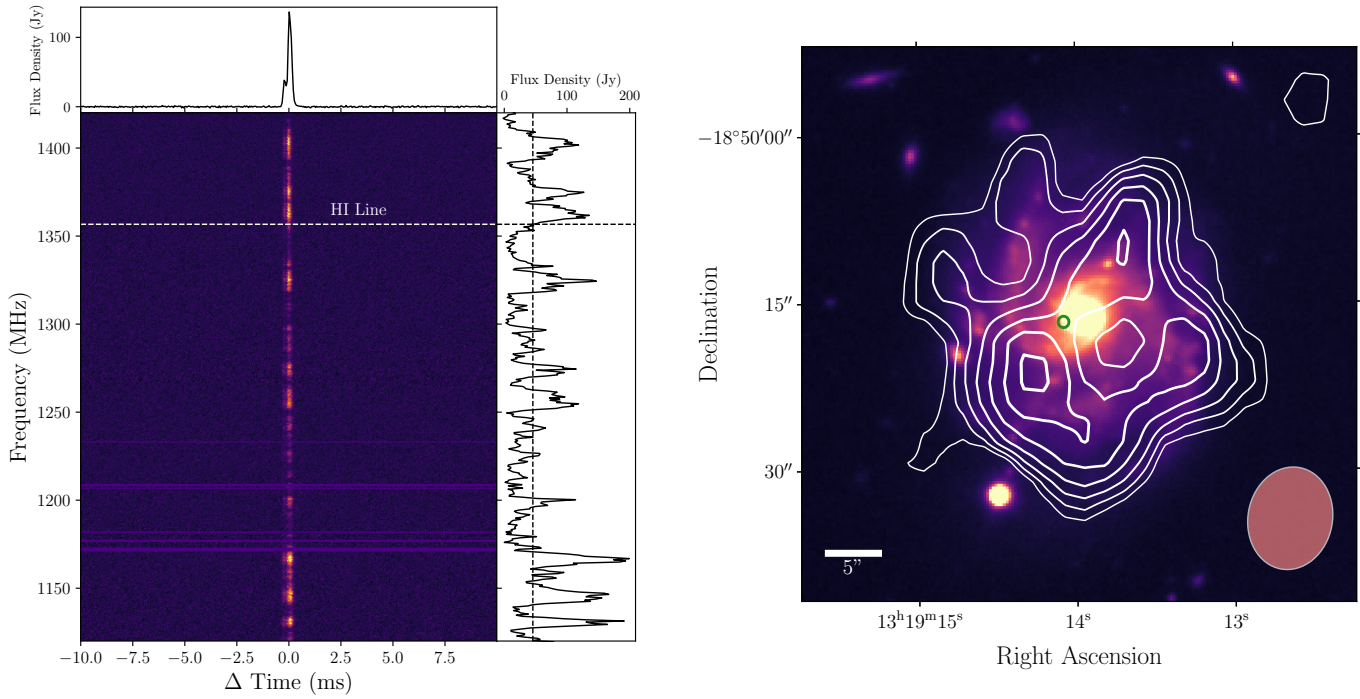


Figure 1. (Left) Dynamic spectrum of FRB 20211127I. The right panel displays the spectrum of the FRB averaged across its temporal pulse width. The location of the redshifted $\text{H}\alpha$ line is shown by the horizontal dashed line, and the band-averaged flux density is denoted by the vertical dashed line in the right panel. (Right) VLT i -band image of the host galaxy of FRB 20211127I overlaid with its $\text{H}\alpha$ emission as seen by MeerKAT (white contours) and the localisation region in green. Contours increase as $[1, 1.25, 1.5, \dots] \times 5.34 \times 10^{20} \text{ cm}^{-2}$ and the beam is shown in the bottom right.

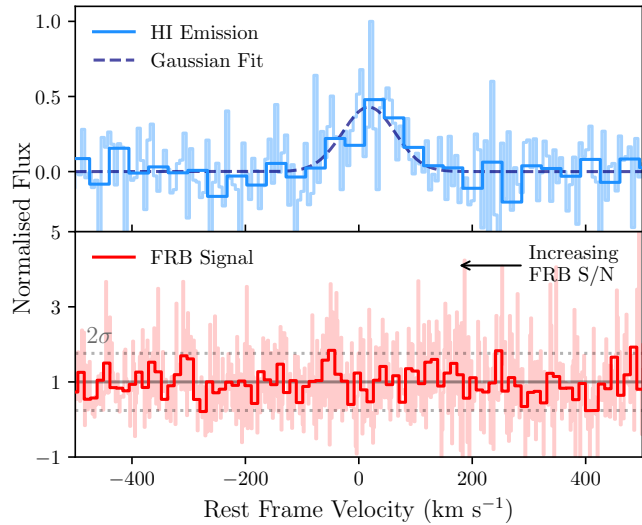


Figure 2. (Top) Normalised $\text{H}\alpha$ emission measured by MeerKAT at the pixel closest to the localisation region. The raw data is overlaid with a Gaussian profile fit to the binned data. (Bottom) Flattened and normalised FRB spectrum at the location of the $\text{H}\alpha$ line. For visual purposes, the spectrum is overlaid with a binned spectrum at a velocity resolution of 11 km s^{-1} in the rest frame and the 2σ deviation from unity is shown. Due to scintillation, the SNR of the spectrum increases towards the left.

4.1 Strengths and Limitations of FRB 20211127I

FRB 20211127I is in many ways an ideal burst for such an investigation. It is a bright and narrow burst, exhibiting little

to no scattering, which allows for a high SNR in the pulse-averaged spectrum. Even the dominant interstellar scintillation pattern noted earlier does not present a major barrier in this case. Scintillation typically complicates absorption searches, and this FRB exhibits one of the strongest patterns in the CRAFT sample; Scott et al. (2025) report a spectral modulation index of $m = 0.74$ (values near unity indicate strong scintillation). Even so, its impact on the effective sensitivity of this test case is minimal. As shown by the FRB spectrum in the left image of Fig. 1, the flux density of the spectrum at the location of the $\text{H}\alpha$ line almost perfectly coincides with the band-averaged flux density of the FRB. As such, our 3σ limit would not change significantly if the scintillation was weaker or even non-existent. In fact, scintillation of this manner could, in a different scenario, be considered an advantage rather than a disadvantage; for FRBs with v_{DC} values significantly larger than the typical width of absorption features, as is the case for FRB 20211127I, a coincidental alignment of a scintle with the $\text{H}\alpha$ line could provide a boost in SNR across the line that could significantly alter the likelihood of detection.

To illustrate this, we consider the resulting limits on both integrated optical depth and T_{spin} were the $\text{H}\alpha$ line to coincide with the local spectral maxima near 1362 MHz, rather than at 1357 MHz. In this case, the SNR increases by roughly a factor of 2, yielding an integrated optical depth limit of approximately 14 km s^{-1} and a corresponding T_{spin} lower limit of 56 K. Such an integrated optical depth is still very much on the extreme boundary of plausible detection (Braun 2012), though the resulting T_{spin} limit would be within ~ 15

K of typical temperatures observed in the Milky Way's CNM (Murray *et al.* 2018).

4.2 Detectability of HI Absorption in Non-repeating FRBs

4.2.1 Current Facility Capabilities

As outlined in Section 2, the detectability of HI absorption in FRB signals is governed by a combination of instrumental and source properties, including the system noise, the HI line width, and the FRB's intensity, temporal duration, and redshift. To understand the broader likelihood of any given facility to detect absorption/constrain T_{spin} , we must also consider their fields of view (FoV) and frequency ranges, as well as the intrinsic luminosity distribution and spectral behaviour of the FRB population.

Although absorption measurements are not limited by the distance-dependent sensitivity constraints that restrict HI emission studies to the local Universe, this method used to constrain T_{spin} relies on the availability of emission maps. For this reason, facilities which do not cover the 1.3–1.42 GHz band where local Universe HI is detected cannot meaningfully contribute to such analysis. We therefore exclude the Canadian Hydrogen Intensity Mapping Experiment (CHIME; Bandura *et al.* 2014) which observes between 400–800 MHz, but note that its successor, The Canadian Hydrogen Observatory and Radio-transient Detector (CHORD; Vanderlinde *et al.* 2019), will operate with an ultra-wide band between 300–1500 MHz and thus is poised to become an important resource for future work. Henceforth, we consider only the current capabilities of the remaining major facilities in the field — ASKAP, the Deep Synoptic Array (DSA; Kocz *et al.* 2019), FAST, and MeerKAT.

Our aim is to estimate the likelihood that a non-repeating FRB detected by each of these facilities will be bright enough to probe realistic HI absorption. By calculating this probability, we can quantify the broader relative ability of these different observatories to conduct such studies. Eq. 10 provides us with the tools to make such estimates; all we require are the SEFDs of the telescopes. Since ASKAP, DSA, and MeerKAT each have the capability to process FRBs offline after detection, we can assume the full sensitivity achievable through coherent beamforming. At current maximum operating capacities (36, 63, and 64 antennas, respectively), their effective SEFDs are approximately 50 Jy, 100 Jy, and 12.5 Jy, while FAST achieves around 1.25 Jy at *L*-band.

Once again setting the absorption line width W to 50 km s $^{-1}$, Figure 3 presents grids of 3σ integrated optical depth limits as a function of burst width and fluence for each telescope. We overlay FRBs with reported widths and fluences to contextualise current samples — the recent sample expansions for DSA (Sharma *et al.* 2024; Connor *et al.* 2025) and MeerKAT (Pastor-Marazuela *et al.* 2025) do not currently include such information — though we note that many of these FRBs were observed with fewer than the maximum number of antennas; in these cases the true limits are higher than those shown here, meaning that these events appear artificially high relative to the displayed limits. The ASKAP FRBs, which are taken from Shannon *et al.* (2024), are observed with smaller bandwidths

than the other facilities, and thus we colour each by their central observing frequencies, noting that many lie outside our near-Universe band of interest. However, this figure indicates that integrated optical depths of a few km s $^{-1}$ are certainly detectable, though only for very high-fluence bursts.

One event stands out clearly in this figure: the MeerKAT FRB 20210405I. This burst was exceptionally bright and was localised to a nearby galaxy at $z \sim 0.06$ (Driessen *et al.* 2023). Follow-up observations by Roxburgh *et al.* (2025) revealed a face-on HI disk in the host galaxy, making this source an excellent candidate for probing HI absorption and constraining the host-galaxy T_{spin} . Unfortunately, the burst was detected prior to the implementation of MeerTRAP's transient buffer system (K. M. Rajwade *et al.* 2024), which now enables the recording of full-voltage data for later processing. Consequently, only a coarse 1024-channel spectrum spanning ~ 800 MHz is available, providing insufficient spectral resolution for a meaningful absorption search. Nonetheless, this event demonstrates that such favourable FRBs do occur, and that similar sources will be accessible to future absorption studies with the voltage-capture capabilities now available on ASKAP, DSA, and MeerKAT.

To calculate the fraction of detected FRBs capable of probing HI absorption, we must define an SNR threshold, $\text{SNR}_{\text{thr}}(w)$, required to surpass a target 3σ integrated optical depth limit, τ_{thr} . We then can estimate the probability $P(\text{SNR} \geq \text{SNR}_{\text{thr}}(w) \mid \text{SNR} \geq \text{SNR}_{\text{det}})$, where SNR_{det} is the detection threshold of the facility. This estimation relies on the SNR distributions observed by each telescope, which reflect the underlying FRB fluence distribution. If this distribution is scale-invariant above each telescope's fluence threshold (F_{det}), all facilities observe SNR distributions of identical shape. Consequently, the fraction of absorption-sensitive bursts scales as $(F_{\text{thr}}(w)/F_{\text{det}})^{\gamma+1}$, where γ is the differential power-law index.

Several studies have attempted to model the fluence distribution of the FRB population (e.g. James *et al.* 2019; Shin *et al.* 2023; Ryder *et al.* 2023; Arcus *et al.* 2025), generally employing a Schechter function to determine the high end cutoff energy imposed by the expected physical limit to the FRB emission mechanism. This function is not scale invariant, but given the downturn must lie orders of magnitude above telescope thresholds (Arcus *et al.* 2025), we can consider the SNR distributions effectively equivalent across instruments. Possible deviations at low fluences — such as variations in the power-law slope reported for some repeaters (Li *et al.* 2021; Kirsten *et al.* 2024) and for non-repeating FRBs detected by MeerKAT (Jankowski *et al.* 2023) — remain inconclusive and are neglected here. Studies in the *L*-band generally find γ values near -2 (James *et al.* 2022; Hoffmann *et al.* 2024; Arcus *et al.* 2025), as expected for a cosmological population of sources. Thus, the fraction of interest reduces simply to $F_{\text{det}}/F_{\text{thr}}(w)$.

As F_{thr} is a function of w , we must multiply this fraction by the probability distribution of pulse widths $p(w)$ and then integrate over w . Ideally we would use each telescope's observed width distribution; due to the current low number of reported widths in DSA, FAST, and MeerKAT, we fit a log normal function to the width distribution of ASKAP and as-

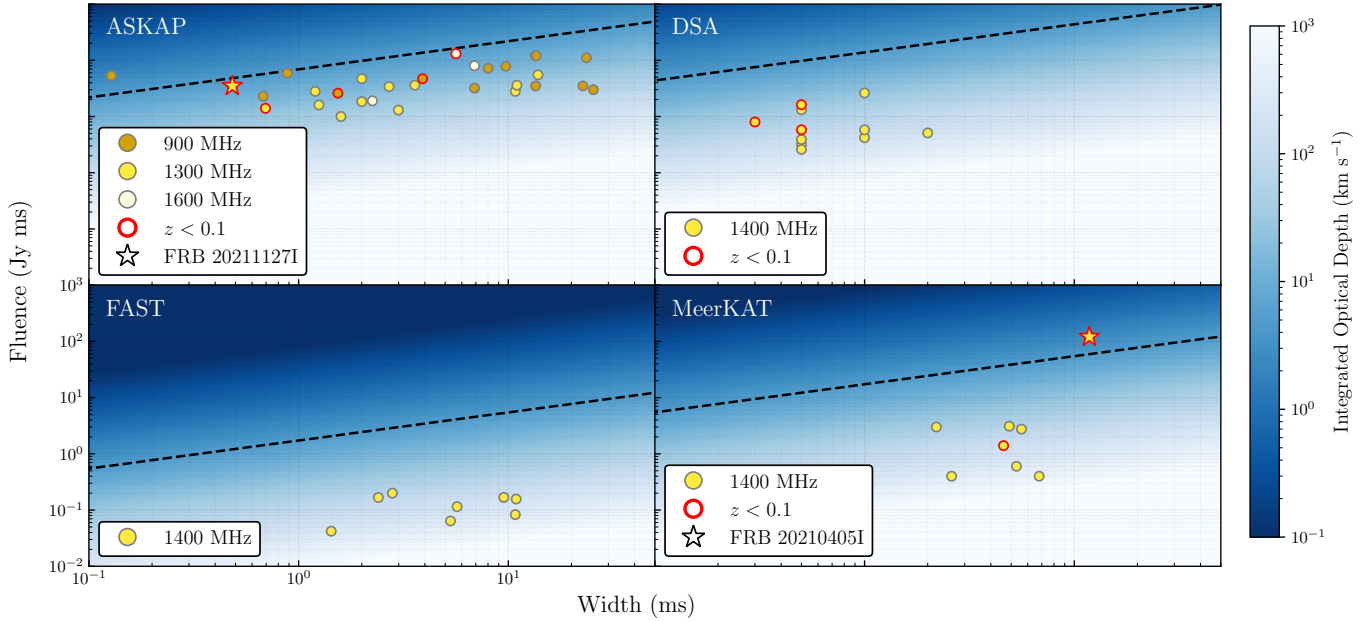


Figure 3. 3σ limits on the integrated $\text{H}\alpha$ optical depth detectable in the pulse-averaged spectra of non-repeating FRBs observed by various telescopes. The black dashed lines in each panel indicate a limit of 5 km s^{-1} . These limits assume maximal sensitivity (i.e. with full antenna configuration) and coherent beamforming, an $\text{H}\alpha$ linewidth of 50 km s^{-1} , and a flat FRB spectrum. Overlaid are samples of reported FRBs with known fluences and widths: ASKAP (Shannon et al. 2024), DSA (Law et al. 2024), FAST (Zhu et al. 2020; Niu et al. 2021; Zhou et al. 2023), and MeerKAT (K M Rajwade et al. 2022; Jankowski et al. 2023; Driessen et al. 2023). ASKAP is divided in colour based on the central frequency of the band used to observe the FRB. In all panels, points with red borders indicate FRBs with known localisations to galaxies with redshifts below 0.1.

sume this for all. Now only the fluence detection thresholds of each telescope and observing system are required (Shannon et al. 2024; Wang et al. 2025; Connor et al. 2025; Niu et al. 2021; Jankowski et al. 2023). As only very bright FRBs can probe low τ_{thr} , such events are detectable even with the incoherent summation modes used by ASKAP and MeerKAT; in these modes, F_{det} is a factor of $\sqrt{N_{\text{ant}}}$ closer to F_{thr} , which doesn't change because it is always defined with respect to the telescopes' coherent sensitivity due to the fact that the array facilities can process offline after detection.

Table 1 presents the resulting absorption-probing fractions of the four observatories in their different detection modes as percentages ($\tau \%$), given a target τ_{thr} of 5 km s^{-1} . From this we can see that a sizeable fraction of FRBs detected with the incoherent modes of ASKAP and MeerKAT are expected to probe realistic $\text{H}\alpha$ absorption. Of course, there are the extra factors concerning the redshift distribution and observation band that further reduce the fraction of usable bursts; however, these numbers indicate that absorption detection in the spectra of FRBs is certainly not implausible.

To compare the relative likelihood of detection between facilities, we must simply estimate the total number of FRBs with fluences greater than F_{thr} each facility will detect in an equal observing time. This figure of merit (FoM) is effectively the total number of FRBs a system detects multiplied by the absorption-probing fractions calculated above. The former is proportional simply to the $\text{FoV} / F_{\text{det}}$, and thus the FoM is given by

Table 1. Comparison of facility-specific sensitivity to $\text{H}\alpha$ absorption. The fourth column indicates the percentage of detected FRBs with fluences great enough to probe an integrated optical depth threshold (τ_{thr}) of 5 km s^{-1} . The Figure of Merit in the final column indicates the relative likelihood of detecting an FRB that probes the same τ_{thr} in an equal observing time, calculated using Eq. 11.

Facility	Detection Mode	F_{det} (Jy ms) ^a	$\tau \%$	$\text{FoV} (\text{deg}^2)$ ^a	FoM
ASKAP	Incoherent	8.0	6.2	30	23.2
	Coherent	1.2	0.9	30	23.2
DSA [†]	Coherent	1.9	0.8	3.4	1.32
FAST	Single dish	0.015	0.5	0.008	0.25
MeerKAT	Incoherent	3.4	10.6	1.3	4.02
	Coherent	0.7	2.0	0.4	1.23

^a Values are taken from Shannon et al. (2024), Wang et al. (2025), Law et al. (2024), Connor et al. (2025), Niu et al. (2021), and Jankowski et al. (2023).

[†] DSA only observes in coherent detection mode.

$$\text{FoM} = \int \frac{\text{FoV}}{F_{\text{thr}}(w)} p(w) \, dw. \quad (11)$$

The resulting values are also found in Table 1. This illustrates that ASKAP, observing in either incoherent or coherent mode, is by far the most likely telescope to probe $\text{H}\alpha$ absorption in the spectra of non-repeating FRBs.

4.2.2 Future Facility Capabilities

Estimating the performance of future facilities like SKA-Mid or the full DSA is challenging, as it depends heavily on the specific configurations of their FRB detection backends. However,

the limits presented in Figure 3 are independent of detection architecture; provided the coherent SEFD of a future facility can be estimated, similar sensitivity projections can be made. The predicted SEFDs for SKA-Mid^a and the 1650-dish DSA^b are approximately 2.5 Jy and 4 Jy, respectively. At these sensitivity levels, a 1 ms burst would require a fluence of 5 Jy ms (SKA-Mid) or 8 Jy ms (DSA) to probe a 50 km s^{-1} wide absorption line at a 3σ integrated optical depth limit of 5 km s^{-1} .

4.3 Repeating FRBs

The population of repeating FRBs poses an entirely different opportunity for probing H α absorption and T_{spin} . Dozens of these sources have now been detected (CHIME/FRB Collaboration *et al.* 2023), with some "hyperactive" repeaters (Konijn *et al.* 2024; Tian *et al.* 2025) exhibiting thousands of outbursts. As these bursts originate from the same environment and traverse identical structures within the host galaxy, stacking their signals increases the cumulative integration time for any imprinted absorption features, effectively boosting the sensitivity to the H α line. This clearly makes hyperactive repeaters — several of which have been localised to host galaxies with redshifts below 0.1 (Day *et al.* 2021; Ravi *et al.* 2023) — the best testing grounds for H α absorption.

With its incredible sensitivity, FAST's true strengths are not in the serendipitous detection of apparently non-repeating FRBs, but in the regular monitoring of these repeating FRBs. If we assume that each burst has the same pulse width (for simplicity; width can vary by an order of magnitude, e.g. Li *et al.* 2021), then the improvement in sensitivity to H α absorption scales with $\sqrt{N_{\text{bursts}}}$. As such, we can estimate how FAST's fluence limit for detecting a given integrated optical depth changes as a function of the number of stacked FRBs, which we demonstrate in Fig. 4. This shows that just 100 FRBs with a pulse width of 1 ms and an average fluence of 2 Jy ms can probe integrated optical depths of just 0.5 km s^{-1} . Of course, we reiterate that this estimate uses idealised, flat spectrum FRBs; however, the $z = 0.077$ repeater FRB 20220912A has outbursted thousands of times with fluences around 1 Jy ms (Zhang *et al.* 2023), and several tens of times above 50 Jy ms (Sheikh *et al.* 2024), indicating that highly sensitive probes of absorption already exist. Furthermore, with CHIME's recent second data release reporting dozens of new repeaters (CHIME/FRB Collaboration *et al.* 2026), the sample of hyperactive repeaters is bound to continue to expand, making absorption detection increasingly realistic.

4.4 FRB Distance Inside Host Galaxy

Fender and Oosterloo (2015) and Margalit and Loeb (2016) previously identified the use of potential H α absorption in FRBs as an independent distance estimator. The rapid improvements in localisation ability since their release have reduced the value

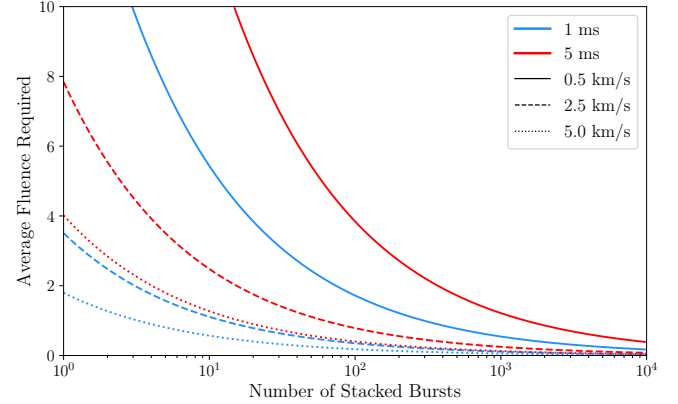


Figure 4. Average burst fluence required for FAST to detect various integrated H α optical depths as a function of the number of bursts stacked from a repeating FRB.

for such a concept. In this paper, we have focused predominantly on using absorption as a tool to measure T_{spin} , but here we briefly comment on another use case that would be of high value to the FRB community. Currently a significant issue facing those who aim to use FRBs as cosmological probes is the unknown contribution of the host galaxy on the dispersion measure (DM) of FRBs (James *et al.* 2022; Connor *et al.* 2025). Disentangling this factor from the cosmological contribution, which is sensitive to several key cosmological parameters, is an ongoing thorn in the side of modellers. Part of this issue arises from the unknowable projected distance an FRB lies within its host; the dispersion of a burst's signal may be significantly larger if it lies on the far side of a galaxy rather than the near side.

If a resolved absorption feature is present in a nearby FRB, it may be possible to compare its location in the band with that of an H α emission line. If the absorption line is blueshifted relative to the emission line, this indicates that the FRB lies on the near side of the bulk of the host's interstellar medium (ISM) or is associated with an intervening cloud. A redshifted feature relative to the emission line would provide strong evidence that the FRB originates on the far side of the galaxy and is seen through the receding half of the local gas column. Comparing this kinematic depth with the measured DM would provide stronger host galaxy constraints than is currently possible. This is particularly critical given the lack of correlation between excess DM and other FRB properties (Marnoch *et al.* in prep.; Scott *et al.* 2025; Mas-Ribas and James 2025), as it would provide a physical rather than statistical basis for DM-host subtractions.

Furthermore, measuring this kinematic depth would provide a direct method to quantify the impact of host galaxy scattering. By definitively placing the FRB relative to the host's H α reservoir, one could determine whether observed pulse broadening is dominated by the dense, turbulent environment immediately surrounding the progenitor or the integrated column of the galactic disk. This distinction is vital for accurately modelling the scattering-DM relation, as it allows us to identify if the host's interstellar medium acts

a. <https://www.skao.int/en/resources/technical-documents>
b. <https://www.deepsynoptic.org/>

as a significant scattering screen or if such effects are largely localised to the source region.

5. Conclusion

We demonstrate a method of constraining the spin temperature of atomic hydrogen gas in galaxies through the comparison of potential H α absorption features in localised FRBs with high resolution H α emission maps. Using the signal of FRB 20211127I, and a 3 hr L -band observation with MeerKAT, we find a 3σ upper limit in the integrated optical depth of 33 km s^{-1} , corresponding to a lower limit on T_{spin} of 26 K. While this non-detection unsurprisingly offers little constraining power, we discuss the possibility of detecting absorption in the signals of FRBs given the capabilities and strategies of modern observatories.

We first calculate the fraction of FRBs detected by ASKAP, DSA, FAST, and MeerKAT capable of probing integrated optical depths below 5 km s^{-1} , finding that the incoherent detection modes of MeerKAT and ASKAP show the greatest proportions at 10% and 6%. By also factoring in FoV and post-detection processing capabilities, we find that ASKAP, observing at full 36-dish strength, currently offers the greatest chance of detecting H α absorption in a non-repeating FRB. This would still require a relatively narrow ($< 3 \text{ ms}$) burst with a fluence greater than 100 Jy ms. However, we reiterate that such FRBs have been previously observed; the $z \sim 0.06$ MeerKAT FRB 20210405I would have probed deep absorption and T_{spin} limits had its voltages been saved to produce a higher resolution spectrum.

We also consider the opportunity presented by the repeating FRB population, particularly the hyperactive sub-population which repeat thousands of times. Monitoring these objects offers a separate avenue that, through FAST's current sensitivity, pushes absorption detection into plausibility through stacking. Finally, we highlight that combining H α absorption with high resolution H α emission maps may provide a way to disentangle the host galaxy contribution to an FRB's dispersion measure from its cosmological contribution, aiding in providing constraining power to cosmological studies using FRBs.

Acknowledgements

We thank Ben Stappers, Laura Driessen, and Adam Deller for providing data and useful discussions that impacted the analysis of this work. H.R. is supported by an Australian Government Research Training Program (RTP) Scholarship. M.G. and C.W.J. acknowledge support by the Australian Government through the Australian Research Council Discovery Projects funding scheme (project DP210102103). A.B. acknowledges support through project CORTEX (NWA.1160.18.316) of the research programme NWA-ORC which is financed by the Dutch Research Council (NWO). M.G. also acknowledges support through UK STFC Grant ST/Y001117/1. For the purpose of open access, the author has applied a Creative Commons Attribution (CC BY) licence to any Author Accepted Manuscript version arising from this submission.

This scientific work uses data obtained from Inyarrimanka Ilgari Bundara, the CSIRO Murchison Radio-astronomy Observatory. We acknowledge the Wajarri Yamaji People as the Traditional Owners and native title holders of the Observatory site. CSIRO's ASKAP radio telescope is part of the Australia Telescope National Facility (<https://ror.org/05qajvd42>). Operation of ASKAP is funded by the Australian Government with support from the National Collaborative Research Infrastructure Strategy. ASKAP uses the resources of the Pawsey Supercomputing Research Centre. Establishment of ASKAP, Inyarrimanka Ilgari Bundara, the CSIRO Murchison Radio-astronomy Observatory, and the Pawsey Supercomputing Research Centre are initiatives of the Australian Government, with support from the Government of Western Australia and the Science and Industry Endowment Fund. We also thank the MRO site staff. The MeerKAT telescope is operated by the South African Radio Astronomy Observatory, which is a facility of the National Research Foundation, an agency of the Department of Science, Technology and Innovation.

References

Allison, James R. 2021. A statistical measurement of the H α spin temperature in DLAs at cosmological distances. *Monthly Notices of the Royal Astronomical Society* 503 (1): 985–996. issn: 13652966. <https://doi.org/10.1093/mnras/stab518>.

Arcus, Wayne R., Clancy James, Ron Ekers, Jean Pierre Macquart, Elaine Sadler, Randall B. Wayth, Keith Bannister, et al. 2025. The fast radio burst population energy distribution. *Publications of the Astronomical Society of Australia* 42. issn: 14486083. <https://doi.org/10.1017/pasa.2024.114>.

Bandura, Kevin, Graeme E. Addison, Mandana Amiri, J. Richard Bond, Duncan Campbell-Wilson, Liam Connor, Jean-François Cliche, et al. 2014. Canadian hydrogen intensity mapping experiment (chime) pathfinder. In *Ground-based and airborne telescopes v*, edited by Larry M. Stepp, Roberto Gilmozzi, and Helen J. Hall, 9145:914522. Society of Photo-Optical Instrumentation Engineers (SPIE) Conference Series. July. <https://doi.org/10.1117/12.2054950>. arXiv: 1406.2288 [astro-ph.IM].

Braun, Robert. 2012. Cosmological evolution of atomic gas and implications for 21cm H α ABSORPTION. *Astrophysical Journal* 749 (1). issn: 15384357. <https://doi.org/10.1088/0004-637X/749/1/87>. arXiv: 1202.1840.

Caleb, Manisha, Themiya Nanayakkara, Benjamin Stappers, Inés Pastor-Marazuela, Ilya S. Khrykin, Karl Glazebrook, Nicolás Tejos, et al. 2025. A fast radio burst from the first 3 billion years of the Universe, arXiv: 2508.01648. <http://arxiv.org/abs/2508.01648>.

CHIME/FRB Collaboration, Thomas Abbott, Bridget C. Andersen, Shion Andrew, Kevin Bandura, Mohit Bhardwaj, Yash Bhusare, et al. 2026. The second chime/frb catalog of fast radio bursts (January). <http://arxiv.org/abs/2601.09399>.

CHIME/FRB Collaboration, Thomas C. Abbott, Daniel Amouyal, Bridget C. Andersen, Shion E. Andrew, Kevin Bandura, Mohit Bhardwaj, et al. 2025. A Catalog of Local Universe Fast Radio Bursts from CHIME/FRB and the KKO. *The Astrophysical Journal Supplement Series* 280, no. 1 (September): 6. issn: 0067-0049. <https://doi.org/10.3847/1538-4365/addbda>. <https://iopscience.iop.org/article/10.3847/1538-4365/addbda>.

CHIME/FRB Collaboration, Mandana Amiri, Bridget C. Andersen, Kevin Bandura, Sabrina Berger, Mohit Bhardwaj, Michelle M. Boyce, et al. 2021. The First CHIME/FRB Fast Radio Burst Catalog. *The Astrophysical Journal Supplement Series* 257 (2): 59. issn: 0067-0049. <https://doi.org/10.3847/1538-4365/ac33ab>. arXiv: 2106.04352.

CHIME/FRB Collaboration, Bridget C. Andersen, Kevin Bandura, Mohit Bhardwaj, P. J. Boyle, Charanjot Brar, Tomas Cassanelli, et al. 2023. CHIME/FRB Discovery of 25 Repeating Fast Radio Burst Sources. *The Astrophysical Journal* 947 (2): 83. ISSN: 0004-637X. <https://doi.org/10.3847/1538-4357/acc6c1>. arXiv: 2301.08762.

Connor, Liam, Vikram Ravi, Kritti Sharma, Stella Koch Ocker, Jakob Faber, Gregg Hallinan, Charlie Harnach, et al. 2025. A gas rich cosmic web revealed by partitioning the missing baryons. *Nature Astronomy* (April). ISSN: 23973366. <https://doi.org/10.1038/s41550-025-02566-y>. arXiv: 2409.16952. <http://arxiv.org/abs/2409.16952>.

Cox, Donald P., and Barham W. Smith. 1974. Large-scale effects of supernova remnants on the galaxy: generation and maintenance of a hot network of tunnels. *The Astrophysical Journal Letters* 189 (May): L105. <https://doi.org/10.1086/181476>.

Curran, S. J., P. Tzanavaris, J. K. Darling, M. T. Whiting, J. K. Webb, C. Bignell, R. Athreya, and M. T. Murphy. 2010. New searches for $\text{H}\alpha$ 21 cm in damped Lyman α absorption systems. *Monthly Notices of the Royal Astronomical Society* 402, no. 1 (February): 35–45. <https://doi.org/10.1111/j.1365-2966.2009.15879.x>. arXiv: 0910.3742 [astro-ph.CO].

Day, Cherie K., Adam T. Deller, Clancy W. James, Emil Lenc, Shivani Bhandari, R. M. Shannon, and Keith W. Bannister. 2021. Astrometric accuracy of snapshot fast radio burst localisations with askap. *Publications of the Astronomical Society of Australia* 38 (September): e050. <https://doi.org/10.1017/pasa.2021.40>. arXiv: 2107.07068 [astro-ph.IM].

Driessen, L N, E D Barr, D A H Buckley, M Caleb, H Chen, W Chen, M Gromadzki, et al. 2023. FRB 20210405I: a nearby Fast Radio Burst localized to sub-arcsecond precision with MeerKAT. *Monthly Notices of the Royal Astronomical Society* 527, no. 2 (November): 3659–3673. ISSN: 0035-8711. <https://doi.org/10.1093/mnras/stad3329>. <https://academic.oup.com/mnras/article/527/2/3659/7337342>.

Driver, Simon P., Stephen K. Andrews, Elisabete Da Cunha, Luke J. Davies, Claudia Lagos, Aaron S.G. Robotham, Kevin Vinsen, et al. 2018. GAMA/G10-COSMOS/3D-HST: The $0 < z < 5$ cosmic star formation history, stellar-mass, and dust-mass densities. *Monthly Notices of the Royal Astronomical Society* 475 (3): 2891–2935. ISSN: 13652966. <https://doi.org/10.1093/mnras/stx2728>. arXiv: 1710.06628.

Farah, W., C. Flynn, M. Bailes, A. Jameson, K. W. Bannister, E. D. Barr, T. Bateman, et al. 2018. Frb microstructure revealed by the real-time detection of frb170827. *Monthly Notices of the Royal Astronomical Society* 478 (1): 1209–1217. ISSN: 13652966. <https://doi.org/10.1093/mnras/sty1122>.

Fender, R., and T. Oosterloo. 2015. Neutral hydrogen absorption towards fast radio bursts. *Monthly Notices of the Royal Astronomical Society: Letters* 451 (1): L75–L79. ISSN: 17453933. <https://doi.org/10.1093/mnrasl/slv065>. arXiv: 1505.01052.

Gatto, A., S. Walch, M.-M. Mac Low, T. Naab, P. Girichidis, S. C. O. Glover, R. Wünsch, et al. 2015. Modelling the supernova-driven ism in different environments. *Monthly Notices of the Royal Astronomical Society* 449, no. 1 (May): 1057–1075. <https://doi.org/10.1093/mnras/stv324>. arXiv: 1411.0009 [astro-ph.GA].

Glowacki, M., A. Bera, K. Lee-Waddell, A. T. Deller, T. Dial, K. Gourdjii, S. Simha, et al. 2024. H i, frb, what's your z : the first frb host galaxy redshift from radio observations. *The Astrophysical Journal Letters* 962 (1): L13. ISSN: 2041-8205. <https://doi.org/10.3847/2041-8213/ad1f62>.

Glowacki, M., K. Lee-Waddell, A. T. Deller, N. Deg, A. C. Gordon, J. A. Grundy, L. Marnoch, et al. 2023. Wallaby pilot survey: h i in the host galaxy of a fast radio burst. *The Astrophysical Journal* 949 (1): 25. ISSN: 0004-637X. <https://doi.org/10.3847/1538-4357/acc1e3>.

Gupta, N., R. Srianand, J. S. Farnes, Y. Pidopryhora, M. Vivek, Z. Paragi, P. Noterdaeme, T. Oosterloo, and P. Petitjean. 2018. Revealing H i gas in emission and absorption on pc to kpc scales in a galaxy at $z \sim 0.017$. *Monthly Notices of the Royal Astronomical Society* 476 (2): 2432–2445. ISSN: 13652966. <https://doi.org/10.1093/mnras/sty384>. arXiv: 1712.03511.

Gupta, Y., B. Ajithkumar, H. S. Kale, S. Nayak, S. Sabhapathy, S. Sureshkumar, R. V. Swami, et al. 2017. The upgraded gmrt: opening new windows on the radio universe. *Current Science* 113, no. 4 (August): 707–714. <https://doi.org/10.18520/cs/v113/i04/707-714>.

Heiles, Carl, and T. H. Troland. 2003. The millennium arecibo 21 centimeter absorption-line survey. ii. properties of the warm and cold neutral media. *The Astrophysical Journal* 586, no. 2 (April): 1067–1093. <https://doi.org/10.1086/367828>. arXiv: astro-ph/0207105 [astro-ph].

Hoffmann, Jordan, Clancy James, Marcin Glowacki, Xavier Prochaska, Alexa Gordon, Adam Deller, Ryan M. Shannon, and Stuart Ryder. 2024. Modelling DSA, FAST, and CRAFT surveys in a z -DM analysis and constraining a minimum FRB energy. *Publications of the Astronomical Society of Australia* 42. ISSN: 14486083. <https://doi.org/10.1017/pasa.2024.127>.

Hopkins, Andrew M., and John F. Beacom. 2006. On the Normalization of the Cosmic Star Formation History. *The Astrophysical Journal* 651 (1): 142–154. ISSN: 0004-637X. <https://doi.org/10.1086/506610>. arXiv: 0601463 [astro-ph.CO].

Hotan, A. W., J. D. Bunton, A. P. Chippendale, M. Whiting, J. Tuthill, V. A. Moss, D. McConnell, et al. 2021. Australian square kilometre array pathfinder: i. system description. *Publications of the Astronomical Society of Australia* 38:1–31. ISSN: 14486083. <https://doi.org/10.1017/pasa.2021.1>. arXiv: 2102.01870.

James, C. W., R. D. Ekers, J. P. Macquart, K. W. Bannister, and R. M. Shannon. 2019. The slope of the source-count distribution for fast radio bursts. *Monthly Notices of the Royal Astronomical Society* 483 (1): 1342–1353. ISSN: 13652966. <https://doi.org/10.1093/mnras/sty3031>.

James, C. W., E. M. Ghosh, J. X. Prochaska, K. W. Bannister, S. Bhandari, C. K. Day, A. T. Deller, et al. 2022. A measurement of Hubble's Constant using Fast Radio Bursts. *Monthly Notices of the Royal Astronomical Society* 516, no. 4 (November): 4862–4881. ISSN: 13652966. <https://doi.org/10.1093/mnras/stac2524>. arXiv: 2208.00819.

Jankowski, F., M. C. Bezuidenhout, M. Caleb, L. N. Driessen, M. Malenta, V. Morello, K. M. Rajwade, et al. 2023. A sample of fast radio bursts discovered and localized with MeerTRAP at the MeerKAT telescope. *Monthly Notices of the Royal Astronomical Society* 524 (3): 4275–4295. ISSN: 13652966. <https://doi.org/10.1093/mnras/stad2041>. arXiv: 2302.10107.

Jonas, Justin L, and The MeerKAT Team. 2016. The meerkat radio telescope pos(meerkat2016)001. *Proceedings of Science*, 1–23. <http://pos.sissa.it/>.

Kanekar, N., J. X. Prochaska, A. Smette, S. L. Ellison, E. V. Ryan-Weber, E. Momjian, F. H. Briggs, et al. 2014. The spin temperature of high-redshift damped Lyman α systems. *Monthly Notices of the Royal Astronomical Society* 438, no. 3 (March): 2131–2166. <https://doi.org/10.1093/mnras/stt2338>. arXiv: 1312.3640 [astro-ph.CO].

Kaur, B., Kanekar N, and J.X. Prochaska. 2025. High-resolution giant metrewave radio telescope hi 21cm imaging of the host galaxy of frb 20250316a. *ArXiv e-Prints* (September): arXiv:2509.04563. <https://doi.org/10.48550/arXiv.2509.04563>. arXiv: 2509.04563 [astro-ph.GA].

Kaur, Balpreet, Nissim Kanekar, and J. Xavier Prochaska. 2022. A fast radio burst progenitor born in a galaxy merger. *The Astrophysical Journal Letters* 925 (2): L20. ISSN: 2041-8205. <https://doi.org/10.3847/2041-8213/ac4ca8>.

Kirsten, F., O. S. Ould-Boukattine, W. Herrmann, M. P. Gawronski, J. W.T. Hessels, W. Lu, M. P. Snelders, et al. 2024. A link between repeating and non-repeating fast radio bursts through their energy distributions. *Nature Astronomy* 8 (3): 337–346. ISSN: 23973366. <https://doi.org/10.1038/s41550-023-02153-z>.

Kocz, J., V. Ravi, M. Catha, L. D'Addario, G. Hallinan, R. Hobbs, S. Kulkarni, et al. 2019. Dsa-10: a prototype array for localizing fast radio bursts. *Monthly Notices of the Royal Astronomical Society* 489 (1): 919–927. ISSN: 13652966. <https://doi.org/10.1093/mnras/stz2219>. arXiv: 1906.08699.

Konijn, David C., Dante M. Hewitt, Jason W. T. Hessels, Ismael Cognard, Jeff Huang, Omar S. Ould-Boukattine, Pragya Chawla, et al. 2024. A nançay radio telescope study of the hyperactive repeating frb 20220912a. *Monthly Notices of the Royal Astronomical Society* 534, no. 4 (November): 3331–3348. <https://doi.org/10.1093/mnras/stae2296>. arXiv: 2407.10155 [astro-ph.HE].

Krumholz, Mark R., Christopher F. McKee, and Jason Tumlinson. 2009. The star formation law in atomic and molecular gas. *The Astrophysical Journal* 699, no. 1 (July): 850–856. <https://doi.org/10.1088/0004-637X/699/1/850>. arXiv: 0904.0009 [astro-ph.GA].

Law, Casey J., Kritti Sharma, Vikram Ravi, Ge Chen, Morgan Catha, Liam Connor, Jakob T. Faber, et al. 2024. Deep Synoptic Array Science: First FRB and Host Galaxy Catalog. *The Astrophysical Journal* 967 (1): 29. issn: 0004-637X. <https://doi.org/10.3847/1538-4357/ad3736>. arXiv: 2307.03344.

Lee-Waddell, Karen, Clancy W. James, Stuart D. Ryder, Elizabeth K. Mahony, Arash Bahramian, Barbel S. Koribalski, Pravir Kumar, et al. 2023. The host galaxy of frb 20171020a revisited. *Publications of the Astronomical Society of Australia* 40:e029. <https://doi.org/10.1017/pasa.2023.27>.

Li, D., P. Wang, W. W. Zhu, B. Zhang, X. X. Zhang, R. Duan, Y. K. Zhang, et al. 2021. A bimodal burst energy distribution of a repeating fast radio burst source. *Nature* 598 (7880): 267–271. issn: 14764687. <https://doi.org/10.1038/s41586-021-03878-5>. arXiv: 2107.08205.

Lorimer, D. R., M. Bailes, M. A. McLaughlin, D. J. Narkevic, and F. Crawford. 2007. A bright millisecond radio burst of extragalactic origin. *Science* 318 (5851): 777–780. issn: 00368075. <https://doi.org/10.1126/science.1147532>. arXiv: 0709.4301.

Madau, Piero, and Mark Dickinson. 2014. Cosmic star-formation history. *Annual Review of Astronomy and Astrophysics* 52:415–486. issn: 00664146. <https://doi.org/10.1146/annurev-astro-081811-125615>. arXiv: 1403.0007.

Margalit, Ben, and Abraham Loeb. 2016. Inferring the distances of fast radio bursts through associated 21-cm absorption. *Monthly Notices of the Royal Astronomical Society: Letters* 460 (1): L25–L29. issn: 17453933. <https://doi.org/10.1093/mnrasl/slw068>.

Mas-Ribas, Lluís, and Clancy W. James. 2025. A τ –DM relation for FRB hosts?, arXiv: 2508.13317. <http://arxiv.org/abs/2508.13317>.

Masui, Kiyoshi, Hsiu Hsien Lin, Jonathan Sievers, Christopher J. Anderson, Tzu Ching Chang, Xuelei Chen, Apratim Ganguly, et al. 2015. Dense magnetized plasma associated with a fast radio burst. *Nature* 528, no. 7583 (December): 523–525. issn: 14764687. <https://doi.org/10.1038/nature15769>. arXiv: 1512.00529.

McKee, C. F., and J. P. Ostriker. 1977. A theory of the interstellar medium: three components regulated by supernova explosions in an inhomogeneous substrate. *The Astrophysical Journal* 218 (November): 148–169. <https://doi.org/10.1086/155667>.

Michałowski, Michał J. 2021. Asymmetric h i 21 cm lines of fast radio burst hosts: connection with galaxy interaction. *The Astrophysical Journal Letters* 920 (1): L21. issn: 2041-8205. <https://doi.org/10.3847/2041-8213/ac2b35>.

Murray, Claire E., Snežana Stanimirović, W. M. Goss, Carl Heiles, John M. Dickey, Brian Babler, and Chang-Goo Kim. 2018. The 21-sponge h i absorption line survey. i. the temperature of galactic h i. *The Astrophysical Journal Supplement Series* 238 (2): 14. issn: 0067-0049. <https://doi.org/10.3847/1538-4365/aad81a>.

Nan, Rendong, D I Li, Chengjin Jin, Qiming Wang, Lichun Zhu, Wenbai Zhu, Haiyan Zhang, Youling Yue, and Lei Qian. 2011. *The five-hundred-meter aperture spherical radio telescope (fast) project*. Technical report. May. <https://doi.org/10.1142/S0218271811019355>.

Niu, Chen-Hui, Di Li, Rui Luo, Wei-Yang Wang, Jumei Yao, Bing Zhang, Wei-Wei Zhu, et al. 2021. CRAFTS for Fast Radio Bursts: Extending the Dispersion–Fluence Relation with New FRBs Detected by FAST. *The Astrophysical Journal Letters* 909 (1): L8. issn: 2041-8205. <https://doi.org/10.3847/2041-8213/abe7f0>. arXiv: 2102.10546.

Pastor-Marazuela, Inés, Alexa C Gordon, Ben Stappers, Ilya S Khrykin, Nicolas Tejos, Kaustubh Rajwade, Manisha Caleb, et al. 2025. Localisation and host galaxy identification of new Fast Radio Bursts with MeerKAT. *Monthly Notices of the Royal Astronomical Society* 27708, no. February (December): 1–19. issn: 0035-8711. <https://doi.org/10.1093/mnras/staf2144>. <https://academic.oup.com/mnras/advance-article/doi/10.1093/mnras/staf2144/8363665>.

Pleunis, Ziggy, Deborah C. Good, Victoria M. Kaspi, Ryan Mckinven, Scott M. Ransom, Paul Scholz, Kevin Bandura, et al. 2021. Fast Radio Burst Morphology in the First CHIME/FRB Catalog. *The Astrophysical Journal* 923 (1): 1. issn: 0004-637X. <https://doi.org/10.3847/1538-4357/ac33ac>. arXiv: 2106.04356.

Prochaska, Jason X., Hsiao-Wen Chen, Arthur M. Wolfe, Miroslava Dessauges-Zavadsky, and Joshua S. Bloom. 2008. On the nature of velocity fields in high- z galaxies. *The Astrophysical Journal* 672 (1): 59–71. issn: 0004-637X. <https://doi.org/10.1086/523689>.

Rajwade, K. M., M. C. Bezuidenhout, M. Caleb, L. N. Driessen, F. Jankowski, M. Malenta, V. Morello, et al. 2022. First discoveries and localizations of fast radio bursts with meertrapp: realtime, commensal meerkat survey. *Monthly Notices of the Royal Astronomical Society* 514, no. 2 (June): 1961–1974. issn: 0035-8711. <https://doi.org/10.1093/mnras/stac1450>. <https://academic.oup.com/mnras/article/514/2/1961/6595347>.

Rajwade, K. M., L. N. Driessen, E. D. Barr, I. Pastor-Marazuela, M. Berezina, F. Jankowski, A. Muller, et al. 2024. A study of two frbs with low polarization fractions localized with the meertrapp transient buffer system. *Monthly Notices of the Royal Astronomical Society* 532 (4): 3881–3892. issn: 13652966. <https://doi.org/10.1093/mnras/stae1652>.

Ravi, Vikram, Morgan Catha, Ge Chen, Liam Connor, Jakob T. Faber, James W. Lamb, Gregg Hallinan, et al. 2023. Deep synoptic array science: discovery of the host galaxy of frb 20220912a. *The Astrophysical Journal Letters* 949 (1): L3. issn: 2041-8205. <https://doi.org/10.3847/2041-8213/acc4b6>. <https://iopscience.iop.org/article/10.3847/2041-8213/acc4b6>.

Reeves, S. N., E. M. Sadler, J. R. Allison, B. S. Koribalski, S. J. Curran, M. B. Pracy, C. J. Phillips, H. E. Bignall, and C. Reynolds. 2016. H α emission and absorption in nearby, gas-rich galaxies ii. — sample completion and detection of intervening absorption in ngc 5156. *Monthly Notices of the Royal Astronomical Society* (January). <https://doi.org/10.1093/mnras/stv3011>. arXiv: 1601.03753. <http://arxiv.org/abs/1601.03753%20http://dx.doi.org/10.1093/mnras/stv3011>.

Roxburgh, H., M. Glowacki, A. Bera, C. W. James, N. Deg, Q. Huang, K. Lee-Waddell, et al. 2025. The distribution of atomic hydrogen in the host galaxies of frbs. *Publications of the Astronomical Society of Australia* (November). issn: 14486083. <https://doi.org/10.1017/pasa.2025.10123>.

Roy, Nirupam, Nissim Kanekar, Robert Braun, and Jayaram N. Chengalur. 2013. The temperature of the diffuse h i in the milky way - i. high resolution h i-21 cm absorption studies. *Monthly Notices of the Royal Astronomical Society* 436, no. 3 (December): 2352–2365. <https://doi.org/10.1093/mnras/stt1743>. arXiv: 1309.4098 [astro-ph.GA].

Ryder, S D, K W Bannister, S Bhandari, A T Deller, R D Ekers, M Glowacki, A C Gordon, et al. 2023. A luminous fast radio burst that probes the Universe at redshift 1. *Science* 382:294–299. <https://www.science.org>.

Scott, D. R., H. Cho, C. K. Day, A. T. Deller, M. Glowacki, K. Gourdji, K. W. Bannister, et al. 2023. Celebi: the craft effortless localisation and enhanced burst inspection pipeline. *Astronomy and Computing* 44 (July). issn: 22131337. <https://doi.org/10.1016/j.ascom.2023.100724>.

Scott, D. R., T. Dial, A. Bera, A. T. Deller, M. Glowacki, K. Gourdji, C. W. James, et al. 2025. High-time-resolution properties of 35 fast radio bursts detected by the commensal real-time askap fast transients survey. *Publications of the Astronomical Society of Australia* (October). ISSN: 14486083. <https://doi.org/10.1017/pasa.2025.10103>.

Shannon, R. M., K. W. Bannister, A. Bera, S. Bhandari, C. K. Day, A. T. Deller, T. Dial, et al. 2024. The commensal real-time askap fast transient incoherent-sum survey. *Publications of the Astronomical Society of Australia* (Dm). ISSN: 14486083. <https://doi.org/10.1017/pasa.2025.8>. <http://arxiv.org/abs/2408.02083>.

Sharma, Krittika, Vikram Ravi, Liam Connor, Casey Law, Stella Koch Ocker, Myles Sherman, Nikita Kosogorov, et al. 2024. Preferential Occurrence of Fast Radio Bursts in Massive Star-Forming Galaxies. *Nature* (September). ISSN: 14764687. <https://doi.org/10.1038/s41586-024-08074-9>. arXiv: 2409.16964. <http://arxiv.org/abs/2409.16964>.

Sheikh, Sofia Z., Wael Farah, Alexander W. Pollak, Andrew P. V. Siemion, Mohammed A. Chamma, Luigi F. Cruz, Roy H. Davis, et al. 2024. Correction to: Characterization of the repeating FRB 20220912A with the Allen Telescope Array. *Monthly Notices of the Royal Astronomical Society* 534, no. 3 (October): 1949–1949. ISSN: 0035-8711. <https://doi.org/10.1093/mnras/stae2184>. <https://academic.oup.com/mnras/article/534/3/1949/7814982>.

Shin, Kaitlyn, Kiyoshi W. Masui, Mohit Bhardwaj, Tomas Cassanelli, Pragya Chawla, Matt Dobbs, Fengqiu Adam Dong, et al. 2023. Inferring the energy and distance distributions of fast radio bursts using the first chime/frb catalog. *The Astrophysical Journal* 944 (1): 105. ISSN: 0004-637X. <https://doi.org/10.3847/1538-4357/acaf06>.

Spitler, L. G., P. Scholz, J. W. T. Hessels, S. Bogdanov, A. Brazier, F. Camilo, S. Chatterjee, et al. 2016. A repeating fast radio burst. *Nature* 531 (7593): 202–205. ISSN: 14764687. <https://doi.org/10.1038/nature17168>.

Swarup, G., S. Ananthakrishnan, V. K. Kapahi, A. P. Rao, C. R. Subrahmanya, and V. K. Kulkarni. 1991. The giant metre-wave radio telescope. *Current Science* 60 (January): 95.

Thornton, D., B. Stappers, M. Bailes, B. Barsdell, S. Bates, N. D. R. Bhat, M. Burgay, et al. 2013. A population of fast radio bursts at cosmological distances. *Science* 341 (6141): 53–56. ISSN: 0036-8075. [https://www.science.org/doi/10.1126/science.1236789](https://doi.org/10.1126/science.1236789).

Tian, J., I. Pastor-Marazuela, K. M. Rajwade, B. W. Stappers, K. Shaji, K. Y. Hanmer, M. Caleb, et al. 2025. MeerKAT discovery of a hyperactive repeating fast radio burst source. *Monthly Notices of the Royal Astronomical Society* 540 (2): 1685–1700. ISSN: 13652966. <https://doi.org/10.1093/mnras/staf793>. arXiv: 2505.08372. <https://doi.org/10.1093/mnras/staf793>.

Tielens, A. G. G. M. 2005. *The physics and chemistry of the interstellar medium*.

Vanderlinde, Keith, Adrian Liu, Bryan Gaensler, Dick Bond, Gary Hinshaw, Cherry Ng, Cynthia Chiang, et al. 2019. The canadian hydrogen observatory and radio-transient detector (chord). In *Canadian long range plan for astronomy and astrophysics white papers*, 2020:28. October. <https://doi.org/10.5281/zenodo.3765414>. arXiv: 1911.01777 [astro-ph.IM].

Wang, Z., K. W. Bannister, V. Gupta, X. Deng, M. Pilawa, J. Tuthill, J. D. Bunton, et al. 2025. The craft coherent (craco) upgrade i: system description and results of the 110-ms radio transient pilot survey. *Publications of the Astronomical Society of Australia* 42 (January). ISSN: 14486083. <https://doi.org/10.1017/pasa.2024.107>.

Wilson, Thomas L., Kristen Rohlfs, and Susanne Hüttemeister. 2013. *Tools of radio astronomy*. 6th ed. Astronomy and Astrophysics Library. Berlin, Heidelberg: Springer. ISBN: 978-3-642-39950-3. <https://doi.org/10.1007/978-3-642-39950-3>.

Wolfire, Mark G., Christopher F. McKee, David Hollenbach, and A. G. G. M. Tielens. 2003. Neutral atomic phases of the interstellar medium in the galaxy. *The Astrophysical Journal* 587, no. 1 (April): 278–311. <https://doi.org/10.1086/368016>. arXiv: astro-ph/0207098 [astro-ph].

Zhang, Yong-Kun, Di Li, Bing Zhang, Shuo Cao, Yi Feng, Wei-Yang Wang, Yuanhong Qu, et al. 2023. FAST Observations of FRB 20220912A: Burst Properties and Polarization Characteristics. *The Astrophysical Journal* 955 (2): 142. ISSN: 0004-637X. <https://doi.org/10.3847/1538-4357/aced0b>. arXiv: 2304.14665.

Zhou, D. J., J. L. Han, W. C. Jing, P. F. Wang, C. Wang, T. Wang, W. Y. Wang, et al. 2023. The FAST Galactic Plane Pulsar Snapshot survey – IV. Discovery of five fast radio bursts. *Monthly Notices of the Royal Astronomical Society* 526 (2): 2657–2664. ISSN: 13652966. <https://doi.org/10.1093/mnras/stad2769>. arXiv: 2309.04826.

Zhu, Weiwei, Di Li, Rui Luo, Chenchen Miao, Bing Zhang, Laura Spitler, Duncan Lorimer, et al. 2020. A Fast Radio Burst Discovered in FAST Drift Scan Survey. *The Astrophysical Journal Letters* 895 (1): L6. ISSN: 2041-8205. <https://doi.org/10.3847/2041-8213/ab8e46>. arXiv: 2004.14029.